The Structural and Electrical Properties of NiCr Alloy for the Bottom Electrode of High Dielectric (Ba,Sr)TiO_3 (BST) Thin Films

Eung-Min Lee and Soon-Gil Yoon*

Department of Materials Engineering, Chungnam National University, Daeduk Science Town, Taejon, 305-764, Korea

E-mail : sgyoon@cnu.ac.kr

(Recevied 7 January 2003, Accepted 6 Februauy 2003)

NiCr alloys are prepared onto poly-Si/SiO_2/Si substrates to replace Pt bottom electrode with a new one for integration of high dielectric constant materials. Alloys deposited at Ni and Cr power of 40 and 40 W showed optimum properties in the composition of $Ni_{1.6}Cr_{1.0}$. The grain size of films increases with increasing deposition temperature. The films deposited at 500°C showed a severe agglomeration due to homogeneous nucleation. The NiCr alloys from the rms roughness and resistivity data showed a thermal stability independent of increasing annealing temperature. The 80 nm thick BST films deposited onto $Ni_{1.6}Cr_{1.0}$/poly-Si showed a dielectric constant of 280 and a dissipation factor of about 5 % at 100 kHz. The leakage current density of as-deposited BST films was about 5 x 10^{-7} A/cm^2 at an applied voltage of 1 V. The NiCr alloys are possible to replace Pt bottom electrode with new one to integrate for high dielectric constant materials.

Keywords : NiCr bottom electrode, BST thin films, rf sputtering, Resistivity

1. INTRODUCTION

Barium strontium titanate, (Ba,Sr)TiO_3 (BST), thin films have received a great deal of attention as a likely candidate for dynamic random access memory (DRAM) applications[1-3]. The direct integration of BST films onto polycrystalline silicon plug for a DRAM capacitor structure has many problems. One of the primary problems is the need to deposit the BST films under oxidizing conditions and to minimize postdeposition thermal treatments under low oxygen partial pressures, as the perovskites are susceptible to reduction. This also limits the choice of electrodes as well as barrier layers for the capacitor stack to either Pt, Ru, or conducting oxides, because insulating oxides formed at the BST-electrode interface will lower the stack capacitance. The choice of electrode structures is very important for both processing and integration.

Ferroelectric thin films are normally fabricated with metal-ferroelectric-metal (MFM) structure using Pt which has been the most commonly used metal electrode. The conductive oxide electrodes, such as IrO_2 [4], RuO_2 [5-6], $YBa_2Cu_3O_7$ (YBCO)[7], (La,Sr)CoO_3 (LSCO)[8] and $SrRuO_3$[9] have been intensively used in the preparation of ferroelectric Pb(Zr,Ti)O_3 (PZT) and $SrBi_2Ta_2O_9$ (SBT) thin film capacitors. The conductive oxide electrodes including Pt, Ru, and Ir metals have the drawbacks of high cost and/or complicated structure for the memory device application. The promising electrode materials are known to be Ni-alloys, which have characteristics of excellent heat- and oxidation-resistance even at high temperature[10-11]. The cheap and simple Ni-alloy electrodes can replace Pt and Ir-based electrodes with a new one for integration of ferroelectric thin films.

In this study, the structural and electrical properties of Ni-alloys as the bottom electrodes for ferroelectric thin films were investigated with deposition parameters. The BST films deposited on the optimum NiCr bottom electrode were investigated for the dielectric properties and leakage current through the observation of BST/NiCr interface.

2. EXPERIMENTAL

NiCr bottom electrodes were prepared on polycrystalline silicon (poly-Si) by dc magnetron

Table 1. Deposition conditions of NiCr alloys by dc sputtering and BST films onto NiCr bottom electrodes by rf magnetron sputtering

	Ni/Cr Electrode	BST Thin Films
Target material	Ni, Cr metal target	Sintered $(Ba_{0.65}Sr_{0.35})TiO_3$
Substrate	poly-Si	Ni-Cr/poly-Si
Base pressure of system	5×10^{-6} torr	5×10^{-6} torr
Working pressure	7 ~ 50 mtorr	10 mtorr
Sputtering power	Ni : 10 ~ 40W Cr : 10 ~ 40W	70W
Sputtering gas($Ar:O_2$)	10 : 0	7 : 3
Deposition temperature	RT ~ 500oC	500oC
Annealing temperature	500, 600, 700oC	

sputtering using multi-target of Ni and Cr metal. In order to eliminate native oxide of the poly-Si, Silicon wafers were etched with the following schedule. Wafers were etched for 10 sec using a HF 2.5 mol % solution and then rinsed with deionized water for 5 min in ultrasonic cleaner. After rinsing, wafers were again etched for 5 sec in the solution in which mole ratio of HF 2.5 mol % solution and C_2H_5OH is one to six. Finally, they were blown with nitrogen (99.9999 % purity). The detailed deposition conditions of NiCr-bottom electrode by dc sputtering and BST films by rf magnetron sputtering are summarized in Table I. The film thickness and the surface morphologies were determined from cross-sectional and surface images by scanning electron microscopy (SEM, AKASHI DS-130C). The surface roughness and the crystal structure of the films were examined by atomic force microscopy (AFM) and x-ray diffraction (XRD), respectively. The film composition was identified by Rutherford back scattering spectroscopy (RBS). The NiCr/BST interface was characterized by Auger electron spectroscopy (AES). The resistivity of electrode structures was measured by electrometer (CMT-SR 1000) using a four-point probe. The dielectric and leakage current properties of Pt/BST/NiCr/poly-Si structures were measured by impedance gain phase analyzer (HP 4194A) and Keithley 617 programmable electrometer, respectively. Pt top electrodes (A = 2.0×10^{-4} cm^2) were deposited through a shadow mask onto the BST thin films by dc magnetron sputtering.

3. RESULTS and DISCUSSION

Figure 1 shows x-ray diffraction patterns of NiCr electrodes deposited at room temperature in 7 mtorr ambient as a function of Ni and Cr dc power. The dc power of Cr was varied from 10 to 40 W in constant Ni power of 40 W. The NiCr electrodes are crystallized even at room temperature irrespective of Ni and Cr dc power. The x-ray peak-position exhibiting the NiCr was slightly shifted depending on the dc power of Cr. At Ni and Cr power of 40 and 40 W, peak position of NiCr was correctly consistent with that of the standard sample. Therefore, all of data were obtained from the 40/40 W dc power of Ni/Cr.

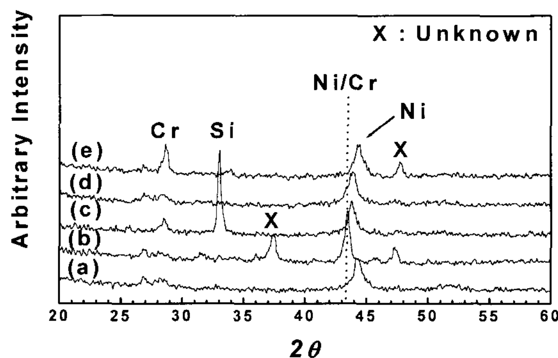

Fig. 1. X-ray diffraction patterns of NiCr alloys deposited at room temperature in 7 mtorr with various Ni/Cr powers of (a) 40/10, (b) 40/30, (c) 40/40, (d) 30/40, and (e) 10/40 W.

Figure 2 shows x-ray diffraction patterns of NiCr deposited at room temperature in dc power of Ni (40W)/Cr(40W) as a function of system pressure. The crystallinity of NiCr decreases with increasing system pressure. Generally, the deposition rate of films by sputtering decreases with increasing above critical system pressure because sputtered atoms or molecules have a short mean-free path and are easily scattered in high pressure ambient[12]. The decrease of film

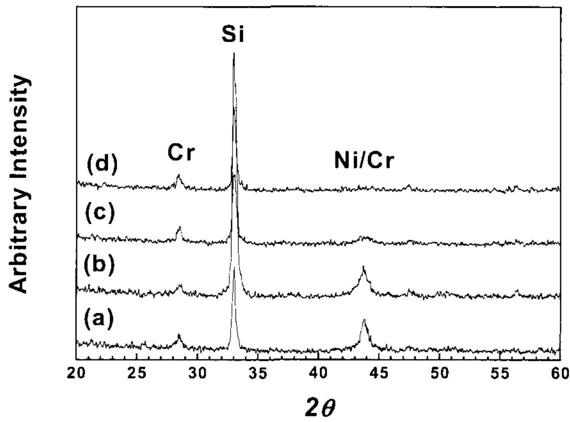

Fig. 2. X-ray diffraction patterns of NiCr alloys deposited at room temperature with Ni/Cr powers of 40/40 W in various system pressures of (a) 7, (b) 10, (c) 30, and (d) 50 mtorr.

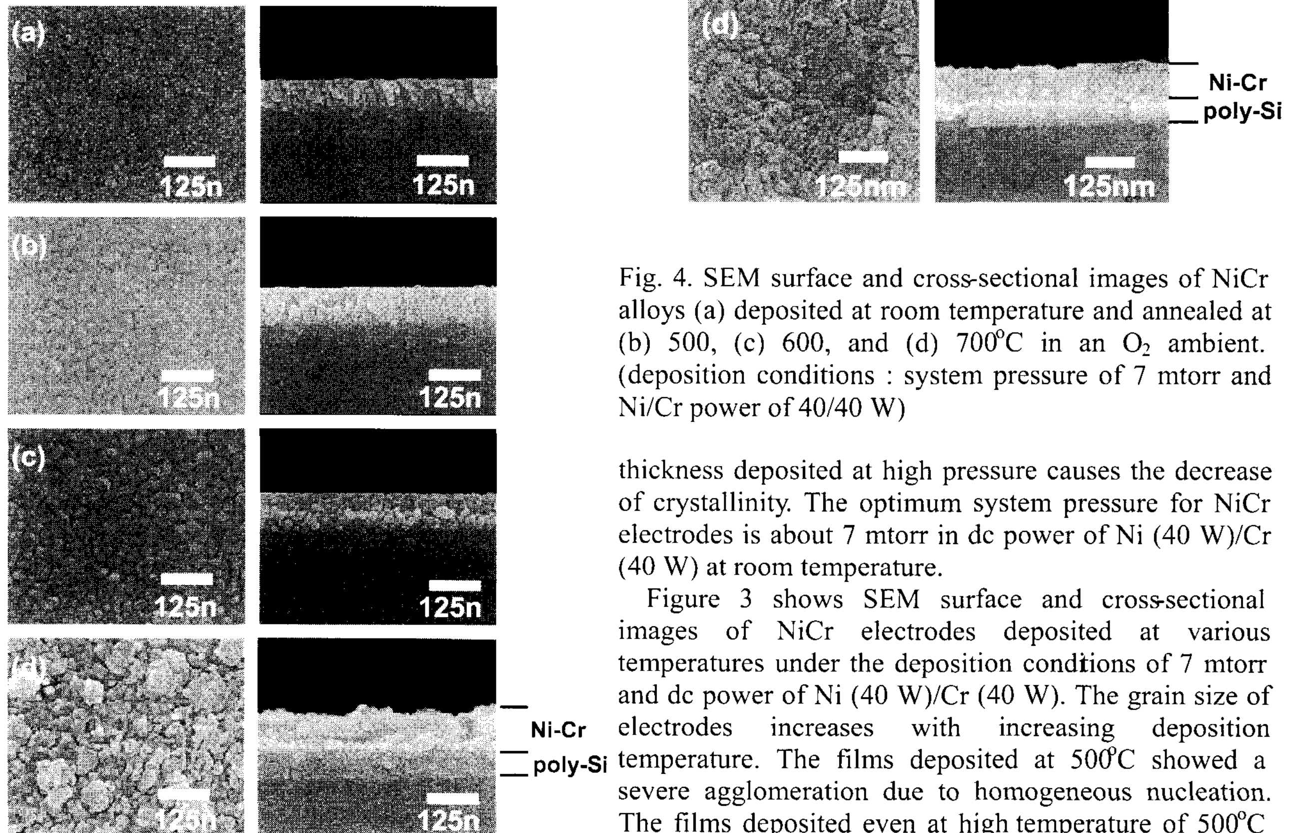

Fig. 3. SEM surface and cross-sectional images of NiCr alloys deposited at various temperatures of (a) room temperature, (b) 200, (c) 400, and (d) 500°C. (deposition conditions : system pressure of 7 mtorr and Ni/Cr power of 40/40 W)

Fig. 4. SEM surface and cross-sectional images of NiCr alloys (a) deposited at room temperature and annealed at (b) 500, (c) 600, and (d) 700°C in an O_2 ambient. (deposition conditions : system pressure of 7 mtorr and Ni/Cr power of 40/40 W)

thickness deposited at high pressure causes the decrease of crystallinity. The optimum system pressure for NiCr electrodes is about 7 mtorr in dc power of Ni (40 W)/Cr (40 W) at room temperature.

Figure 3 shows SEM surface and cross-sectional images of NiCr electrodes deposited at various temperatures under the deposition conditions of 7 mtorr and dc power of Ni (40 W)/Cr (40 W). The grain size of electrodes increases with increasing deposition temperature. The films deposited at 500°C showed a severe agglomeration due to homogeneous nucleation. The films deposited even at high temperature of 500°C have a clear interface between NiCr and poly-Si. The SEM surface and cross-sectional images of films as-deposited at room temperature and annealed at various temperatures are shown in Fig. 4. The samples annealed at 500°C in oxygen ambient had a typical surface morphology due to the oxidation of Cr in the grain boundary (as shown in XRD patterns of Fig. 5) and

showed a severe intermixing at interface between NiCr and poly-Si. A severe interdiffusion at interface after annealing at high temperature was due to the relief of compressive stress formed in as-deposited films by sputtering. The samples annealed at 700°C showed a

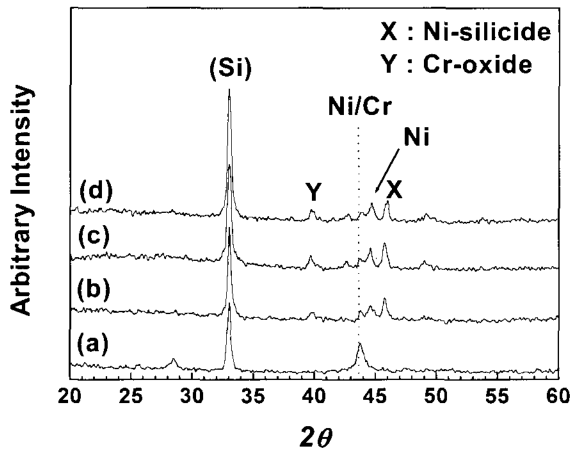

Fig. 5. X-ray diffraction patterns of NiCr alloys (a) deposited at room temperature and annealed at (b) 500, (c) 600, and (d) 700°C in an O_2 ambient.

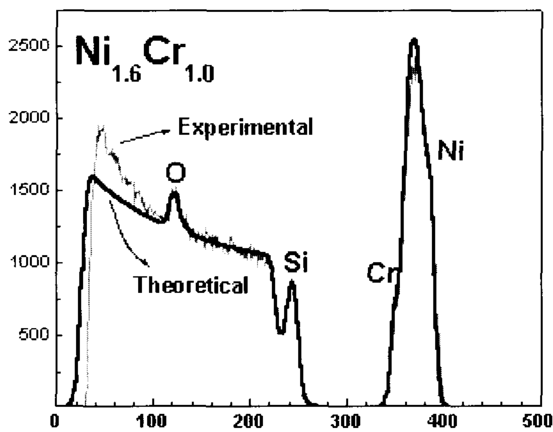

Fig. 6. RBS spectrum of NiCr alloys deposited at room temperature in 7 mtorr with Ni/Cr power of 40/40 W.

abrupt increase of grain size, as compared with samples annealed below 700°C. The NiCr electrodes deposited at room temperature in 7 mtorr and dc power of Ni (40 W)/Cr (40 W) have the composition of $Ni_{1.6}Cr_{1.0}$ from the RBS spectrum shown in Fig. 6.

Figure 7 shows the variation of the roughness and resistivity of NiCr electrode with annealing temperature. The rms (root mean square) roughness of NiCr electrode slightly increases with increasing annealing temperature. The absolutely large roughness of NiCr electrode deposited onto poly-Si was due to the large roughness (rms roughness : around 3.5 nm) of 100 nm thick poly-Si substrate used for NiCr deposition. These results suggested that the roughness of deposition layer was greatly influenced by that of substrate. The NiCr electrode as-deposited at room temperature showed a large resistivity compared with that of samples annealed at various temperatures. The resistivity of samples annealed at 500°C abruptly decrease and slightly increase with increasing annealing temperature. The resistivity of conducting materials depends on the product of carrier mobility and carrier concentration. The carrier mobility is inversely proportional to the film roughness, and the carrier concentration is proportional to the grain size[13]. The roughness of NiCr with increasing annealing temperature up to 700°C showed only a slight increase, compared with the as-deposited electrode. The grain size of NiCr also showed a slight increase with increasing annealing temperature. From this result, resistivity of NiCr is seen not to significantly vary with increasing annealing temperature, if NiCr is not affected from the barrier layers. On the contrary, as-deposited NiCr showed a large resistivity even though samples showed similar roughness to annealed samples. The films deposited at room temperature by sputtering showed less dense structure and smaller grain size than those deposited or annealed at high temperatures. Therefore, the NiCr electrodes deposited at room temperature had a high resistivity. The NiCr electrodes

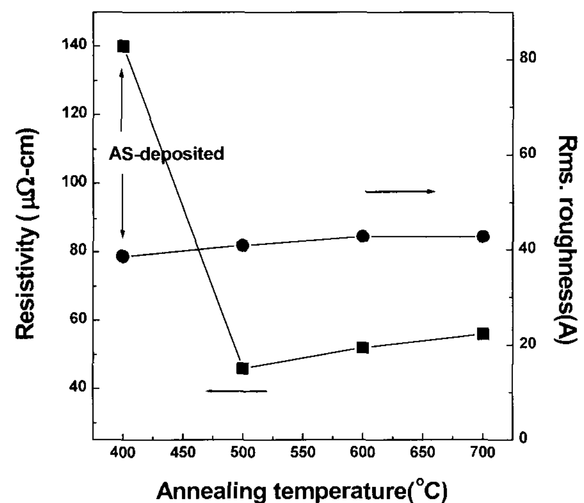

Fig. 7 The rms roughness and resistivity of NiCr alloys annealed at various temperatures in an O_2 ambient. ((deposition conditions : as-deposited at room temperature, system pressure of 7 mtorr and Ni/Cr power of 40/40 W)

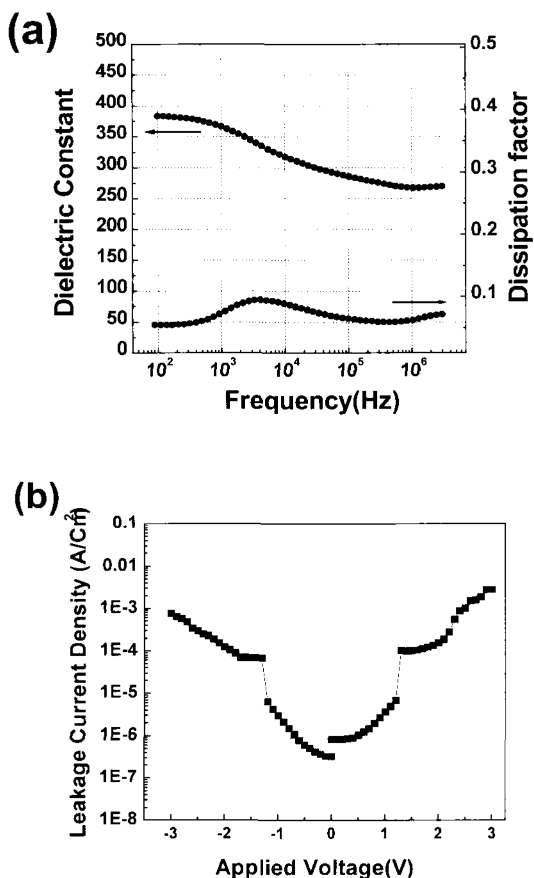

Fig. 8. (a) Dielectric properties vs. frequency and (b) leakage current density vs. applied voltage of BST thin films deposited onto NiCr bottom electrode at 500°C.(deposition conditions of NiCr : system pressure of 7 mtorr and Ni/Cr power of 40/40 W at 400°C)

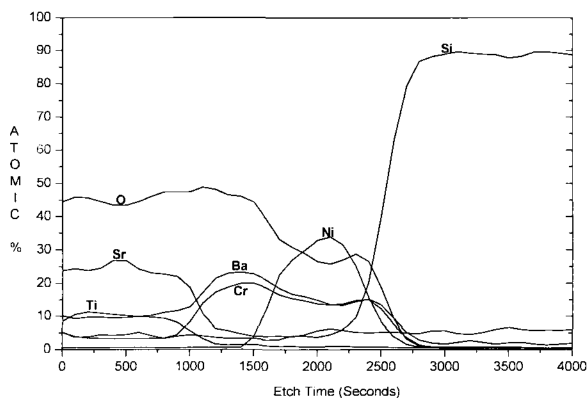

Fig. 9. AES depth-profile for the interface characteristics in BST/NiCr/Si structures. (deposition conditions of NiCr : system pressure of 7 mtorr and Ni/Cr power of 40/40 W at 400°C)

annealed even at 700°C in O_2 ambient after deposition at room temperature have a low resistivity of about 55μ Ω-cm that is enough to apply for integration of high dielectric constant capacitor.

Figures 8 (a) and (b) show the dielectric properties and leakage current behavior of 80 nm thick BST thin films as-deposited at 500°C onto NiCr/poly-Si substrates by rf sputtering. As shown in Fig. 8 (a), dielectric constant of BST films slightly decreased with increasing an applied frequency and dissipation factor was maintained approximately 5% for the increase of applied frequency. As-deposited BST films on NiCr electrodes have a dielectric constant of 280 and a dissipation factor of 5 % at an applied frequency of 100 kHz. The leakage current of BST films showed a symmetric behavior for positive and negative bias voltage without top electrode annealing. The leakage current density of as-deposited BST films was about 5 x 10^{-7} A/cm^2 at an applied voltage of 1 V.

Figure 9 shows the characteristics of NiCr/BST interface using an AES depth-profile. During deposition of BST at 500°C in an O_2 ambient, Cr diffused on the NiCr surface reacts with Ba in BST films and forms approximately 30 nm thick interface between BST and NiCr. The formation of interface produces the Ba deficient BST films and then degraded the dielectric and leakage properties of BST films. The further experiments need to be performed to prevent the diffusion of chromium to NiCr surface at high temperature in an O_2 ambient.

4. CONCLUSION

NiCr alloys deposited at Ni and Cr power of 40 and 40 W showed the optimum properties in the composition of $Ni_{1.6}Cr_{1.0}$. The grain size of electrodes increases with increasing deposition temperature. The films deposited at 500°C showed a severe agglormeration due to homogeneous nucleation. The NiCr alloys from the rms roughness and resistivity data showed a thermal stability independent of increasing annealing temperature. The BST films deposited onto $Ni_{1.6}Cr_{1.0}$/poly-Si showed a dielectric constant of 280 and a dissipation factor of approximately 5 % at 100 kHz. The leakage current density of as-deposited BST films was about 5 x 10^{-7} A/cm^2 at an applied voltage of 1 V. The Ba deficient BST films by the interface formation between NiCr and BST films showed the degraded dielectric and leakage properties. The cheap NiCr alloys are possible to replace Pt bottom electrode with new one to integrate for high dielectric constant materials.

ACKNOWLEDGMENTS

This work was funded by Center for Ultra-microchemical Process Systems sponsored by KOSEF.

REFERENCES

[1] S. G. Yoon, J. C. Lee, and A. Safari, "Preparation of thin film $(Ba_{0.5}Sr_{0.5})TiO_3$ by the laser ablation technique and electrical properties", J. Appl. Phys., Vol. 76, p. 2999, 1994.

[2] S. G. Yoon and A. Safari, "$(Ba_{0.5}Sr_{0.5})TiO_3$ thin film preparation by rf magnetron sputtering and its electric properties", Thin Solid Films, Vol. 254, p. 211, 1995.

[3] W. J. Lee, S. G. Yoon, and H. G. Kim, "Microstructure dependence of electrical properties of $(Ba_{0.5}Sr_{0.5})TiO_3$ thin films deposited on $Pt/SiO_2/Si$", J. Appl. Phys., Vol. 80, p. 5891, 1996.

[4] T. Nakamura, Y. Nakao, A. Kamisawa, and H. Takasu, "Preparation of $Pb(Zr,Ti)O_3$ thin films on Ir and IrO_2 electrodes", Jpn. J. Appl. Phys., Vol. 33, p. 5207, 1994.

[5] S. H. Kim, D. J. Kim, J. G. Hong, S. K. Streiffer, and A. I. Kingon, "Imprint and fatigue properties of chemical solution derived $Pb_{1-x}La_x(Zr_yTi_{1-y})_{1-x/4}O_3$", J. Mater. Res., Vol. 14, p. 1371, 1999.

[6] D. K. Choi, J. Y. Choi, J. H. Won, and S. H. Paek, "Microstructural control of RuO_2 electrode and the related properties of $(Ba,Sr)TiO_3$ thin films", Mat. Res. Soc. Symp. Proc., Vol. 433, p. 45, 1996.

[7] C. S. Chern, S. Liang, Z. Q. Shi, S. G Yoon, A. Safari, P. Lu, B.H. Kear, B. H. Goodreau, T. J. Marks, and S. Y. Hou, "Heteroepitaxial growth of $Ba_{1-x}Sr_xTiO_3/YBa_2Cu_3O_{7-x}$ by plasma-enhanced metalorganic chemical vapor deposition", Appl. Phys. Lett., Vol. 64, p. 3181, 1994.

[8] S. Aggarwal, S. R. Perusse, B. Nagaraj, and R. Ramesh, "Oxide electrodes as barriers to hydrogen damage of $Pb(Zr,Ti)O_3$-based ferroelectric capacitors", Appl. Phys. Lett., Vol. 74, p. 3023, 1999.

[9] K. Wasa, Y. Ichikawa, H. Adachi, I. Kanno, K. Setsune, D. G. Schlom, S. Trolier-Mckinstry, Q. Gan, and C. B. Eom, "Interfacial structure and ferroelectric properties of $PZT/SrRuO_3$ heterostructures on MISCUT (001) $SrTiO_3$", Integr. Ferroelectr., Vol. 26, p. 39, 1999.

[10] T. Ogawa, S. Shindou, A. Senda, and T. Kasanami, "Ferroelectricity of lanthanum-modified lead-titanate thin films deposited on nickel alloy electrodes", Mat. Res. Soc. Symp. Proc., Vol. 243, p. 93, 1992.

[11] T. Ogawa, "Ceramic electronic component and method of fabricating the same", U. S. Patent 5088002, 1992.

[12] J. A. Thornton, in "Thin Film Processes", eds. J. L. Vossen and W. Kern, Academic Press, New York, 1978.

[13] W. C. Shin and S. G. Yoon, "Characterization of RuO_2 thin films prepared by hot-wall metalorganic chemical vapor deposition", J. Electrochem. Soc, Vol. 144, p.1055, 1997.